Journal of Engineering Sciences
Vol 10, Issue 9, Sept /2019
ISSN NO:0377-9254

AN IMPLEMENTATION OF THREE-PHASE HYBRID CONVERTER FOR A PV CHARGING STATION

[1]CH.SURESH KUMAR, [2]N.S.KALYAN CHAKRAVARTHI

[1]M.Tech Student, [2]Assistant Professor

Department of EEE,

KAKINADA INSTITUTE OF TECHNOLOGICAL SCIENCES (KITS), RAMACHANDRAPURAM

ABSTRACT: Hybrid boost converter (HBC) has been proposed to replace a dc/dc boost converter and a dc/ac converter to reduce conversion stages and switching loss. In this paper, control of a three-phase HBC in a PV charging station is designed and tested. This HBC interfaces a PV system, a dc system with hybrid plug in electrical vehicles (HPEVs) and a three-phase ac grid. The control of the HBC is designed to realize maximum power point tracking (MPPT) for PV, dc bus voltage regulation, and ac voltage or reactive power regulation. A test bed with power electronics switching details is built in MATLAB /Sim Power systems for validation. Simulation results demonstrate the feasibility of the designed control architecture. Finally, lab experimental testing is conducted to demonstrate HBC's control performance.

Index Terms—Plug-in hybrid vehicle (PHEV), Vector Control, Grid-connected Photovoltaic (PV), Three-phase Hybrid Boost Converter, Maximum Power Point Tracking (MPPT), Charging Station.

1. INTRODUCTION

The environmental and economic advantages of PHEV lead to the increase in number of production and consumption [1]. The U.S. Department of Energy forecasts that over one million PHEVs will be sold in the U.S. during the next decade [2]. Research has been conducted on developing a charging station by integrating a three-phase ac grid with PHEVs [3]–[5]. The comparison of different PHEV chargers' topologies and techniques are reviewed in [1], [6]. However, a large-scale penetration of PHEVs may add more pressure on the grid during charging periods. Therefore, charging stations with PV as an additional power source become a feasible solution.

For PV charging stations, [7] proposed an architecture and controllers. The charging management is developed in [8] by considering the grid's loading limit. For this type of systems, it requires controlling at least three different power electronic converters to charge PHEVs. Each converter needs an individual controller, which increases complexity and power losses of the system. Consequently, it is urgent to investigate multi-port converters to reduce the number of converting stages. The objective of the paper is to implement such a multi-port converter in a PV charging station for PHEVs and design the controller.

This paper proposes control design and power management for a PV charging station for PHEV by use of a three-phase HBC. The PV charging station charges PHEVs using power from PV and/or the ac grid. The three-phase HBC integrates three main elements of the system: PV, PHEV and the grid. Control design will be presented in detail. The control will enable PV maximum power point tracking (MPPT) and dc voltage control regulation for PHEVs.

Our contributions lie in two aspects. The first contribution is modeling of a PV charging station based on a three-phase HBC that integrates PV arrays, PHEVs, and a utility grid. This novel topology of PV charging station, to the best of authors' knowledge, has not yet been seen in the literature. The advantage of the HBC based PV charging station is the reduction of the number of power conversion stages and losses. The existing PV charging station requires controlling at least three converters including a dc boost converter for MPPT algorithm, a three-phase dc/ac inverter, and a dc converter for battery's charging [8]. Instead, the HBC integrates the first dc boost converter and the dc/ac three-phase inverter into a single structure.

The second contribution is the design of the HBC controller. Existing controllers for HBC [9]–[10] have not included MPPT function since the dc input side is assumed as a stiff dc voltage in the aforementioned research. In our research, we consider the details related to the PV and further implemented MPPT algorithm in an HBC.

2.SYSTEM CONFIGURATION

A three-phase HBC uses the same amount of switches as a two-level voltage source converter (VSC). However, the HBC can realize both dc/dc conversion and dc/ac conversion. As a comparison, Fig. 1 shows the conventional PV charging station where a dc/dc boost converter and a three-phase VSC are used to integrate the PV system, the PHEVs and the ac grid. A three-phase HBC replaces the two converters: the dc/dc boost converter and the dc/ac three-phase VSC to decrease the energy conversion stages and the power losses of the PV charging station. Fig. 2 shows the HBC-based PV charging station's topology. The main components of the configuration of the PV charging station

consist of PV array, three-phase bidirectional HBC, ac grid, off-board dc/dc converter, and PHEV's batteries.

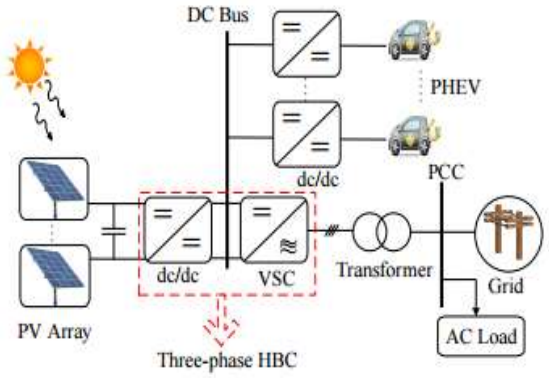

Fig. 1. Architecture configurations of a PV charging station. The conventional topology includes a dc/dc converter and a dc/ac VSC. These two converters will be replaced by a three-phase HBC.

In order to design the control of a PV charging station, it is essential to understand the operation of a three-phase HBC. Detailed operation of an HBC can be found in [11], [12], [17]. Here a brief description is given. The system is composed of a PV array, a dc system, a three-phase ac system, and the interfacing three-phase HBC as shown in Fig. 2. The PV side includes a large inductance to achieve continuous condition and capacitance to decrease the voltage ripple. The dc side includes a diode, a dc bus for PHEV connection, a dc capacitor to eliminate the output current ripples, an off-board unidirectional isolated dc/dc converter, and PHEV batteries. The ac system includes a three-phase LC filter, a step-up transformer, and the point of common coupling (PCC) bus that connects the PV station to the main grid.

The PV array is composed of connecting series cells and parallel strings. Each PV cell has specific characteristics depending on the type and designing criteria. PV models depend mainly on Shockley diode equation . PV can be modeled as a photon-generated current source in parallel with a two-diode system and a shunt resistor, Rsh, as well as in series with a series resistor, Rs. The mathematical equations of two-diode PV cell are given in [18]. HBC-based PV charging station has the capability to operate at medium and high power ratings of such PV power plants since a single IGBT-based VSC has the capability to operate at high voltage rating (e.g., voltage limitation up to1200 V [19]).

Traditional dc/dc boost converter is operated on two modes which are "on" and "off" states. Conventional VSC is operated on "active" and "zero" modes where the output ac power can have a value or zero. The three-phase HBC integrates the operational phases of a VSC and a dc/dc converter into three main modes. The main three intervals include a shoot-through (ST) mode, an active mode (A), and a zero mode (Z).

Some assumptions are considered to better illustrate the steady-state operation of the three-phase HBC. First, the system is assumed to be lossless where the damping elements equal zero. Second, the voltage drop on the diode is very small so it can be ignored. Next, the operational mode of the three phase HBC is operated as an inverter where the power flows from the PV into the grid. It is recognized that the three phase HBC can be operated at converter or inverter based on the direction of power flow. Finally, the diode current is continuous during the active phase. The steady-state relations between the PV, the dc side and the ac side are given as follows.

$$V_{\rm dc} = \frac{V_{\rm pv}}{1 - D_{st}}, \quad \hat{V}_{\rm ac} = M_i \frac{V_{\rm dc}}{2}$$

$$V_{LL} = M_i \frac{\sqrt{3}}{\sqrt{2}} \frac{V_{\rm dc}}{2} = 0.612 \frac{M_i}{1 - D_{st}} V_{\rm pv}$$

where Mi and Dst are the ac voltage per-phase modulation index and duty cycle of the shoot-through period, Vdc, Vˆ ac, and VLL are the peak dc voltage, peak per-phase ac voltage, the RMS value of the line-to-line output ac voltage, respectively. It can be concluded from (2) that the dc output depends on only Dst while ac output depends on both Dst and Mi . In order to achieve continuous control of modified PWM, the controlling signals have to achieve this condition:

$$M_i + D_{st} < 1$$

3.CONTROL STRATERGY

A. Modified PWM

It is mentioned in Section II that the three-phase HBC is operated at three main intervals which are integrated between boost converter and VSC's phases. Conventional sinusoidal PWM and dc PWM are not appropriate to operate the switching states of three-phase HBC. Instead of separately controlling the dc and ac outputs using the switches of three phase HBC, a modified PWM is applied to control two outputs at the same time as shown in Fig. 3. It is recommended to insert the shoot-through phase within the zero mode where the output ac power equals zero in this phase [20]. During the shoot-through period, one leg of the two switchings, e.g., S1 and S4 are both on. This leads to PV side current flowing into S1, S4 only. During the shoot-through period, the inductor L gets charged. At the zero mode, all upper-level switches S1, S3 and S5 are on while the lower-level switches S4, S6 and S2 are off. At this mode, the PV side current all flows to the dc side battery systems while the current to the ac system is zero. Finally, during the active mode, current will flow into the ac system.

The behavior of the open-loop control scheme for switching states of the three-phase HBC is shown in Fig. 3 when the reference for the phase voltages are related as Va > Vb > Vc. The shoot-through operation occurs when the positive signal Vst is lower than carrier signal (phase C is shoot through with S5 and S2) and when the negative signal Vst is

greater than the carrier signal (phase A is shoot-through with S1 and S4 on).Shoot through happens at the phases with the highest voltage or lowest voltage. In Fig. 3, phase A and Phase C are the phases with shoot-through periods. Modified PWM regulates the switching states by controlling five signals which are three-phase ac signals Va, Vb, Vc, and dc signals Vst (Vst = 1 − Dst), and −Vst. The ac controlling signals Va, Vb, and Vc are controlled by modulation index Mi as well as phase angles while the dc signals +Vst, and −Vst are regulated by duty ratio Dst. The advantage of using modified PWM is that both dc and ac outputs can be adjusted.

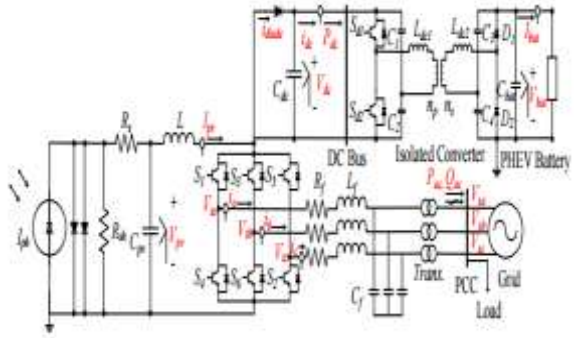

Fig. 2. Topology of the three-phase HBC-based PV charging station.

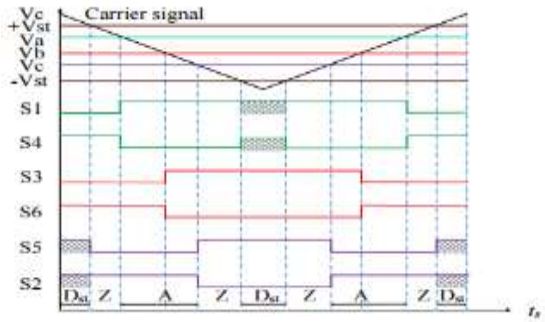

Fig. 3. A modified PWM for the three-phase-HBC. Shoot-through occurs when both switches are closed. ST, A, and Z are shoot-through, active, and zero periods, respectively.

B. control of pv charging station

This section provides a detailed explanation on the framework and controller of the HBC-based PV charging station. From the steady-state relationship in (2), three-phase HBC utilizes Dst to boost the PV voltage while the modulation index Mi regulates the ac voltage Vt's magnitude. In addition, the angle of the three-phase ac voltage Vt can be adjusted to achieve active power and reactive power regulation. When the ac voltage is balanced and the ac system is symmetrical, the total three-phase instantaneous power is constant at steady state. Thus, average power of the ac side equals to the net power at the dc side (Pac = Ppv − Pdc). Three main control blocks are used to control the three phase HBC: MPPT, phase-locked loop (PLL) and vector control as shown in Fig. 4. Each block will be described by a subsection. The charging algorithm of the off-board isolated dc/dc converter will also be addressed in this section.

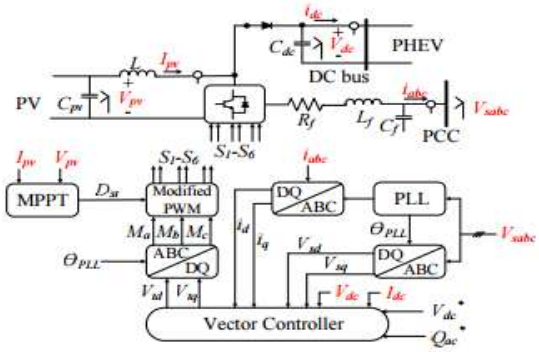

Fig. 4. Control blocks of the HBC-based PV charging station.

C. MPPT

Maximum power point tracking (MPPT) algorithm is important to guarantee maximum power extraction from PV arrays. Various types of MPPT algorithms have been recently applied to control of MPP of PV modules. Hill climbing (HC), perturb and observe (PO), and incremental conductance (IC) are the most attractive algorithms. MPPT techniques with simple structures and fast dynamic performances are demanded. IC among other MPPT methods has the benefits of fast dynamic performance [14], [21]. IC method computes the sensitive of power variation against the PV voltage. The optimal point is achieved when dPpv dVpv = 0. Fig. 5 presents current/voltage relationship and power/voltage relationship for a PV model based on Sun power SPR-E20- 327 which includes 60 parallel strings and 5 series modules in each string to generate maximum power of 100 KW. In the power/voltage plots, the maximum power points (MPPs) are located at the top of each plot when the gradient is zero. The slope is positive in the left hand side of a MPP and negative in the right hand side as shown in Fig. 5.

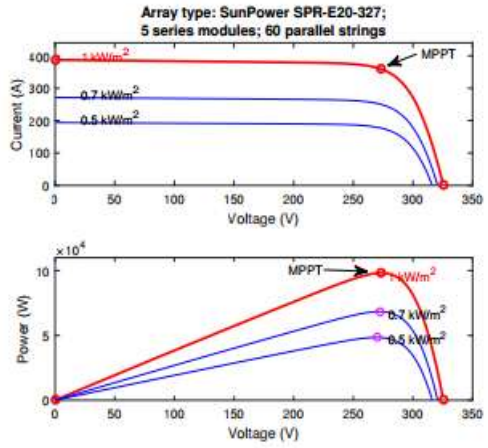

Fig. 5. IV-curve for Sunpower SPR-E20-327. (a) I-V curve. (b) P-V curve. MPP occurs at I_{mpp} = 365 A and V_{pv} = 273.5 V to generate maximum power 100 kW.

D. Vector Control

Vector control technique is used for VSCs. The inner loop controls the ac current while the outer loop controls the dc

voltage and reactive power. The dynamic equations of the three-phase HBC are similar to those of the conventional VSC . The main difference of HBC is the consideration of Dst.

The inner current control loop is designed to respond much faster than the outer voltage controller for fast response and disturbance rejection. It is suggested to achieve fast transient response that the response of the inner loop to be in milliseconds, while the outer loop is 10 times slower than the inner loop.

The open-loop of the inner current loop includes the transfer function of the plant and the delay of the modified PWM as well as the PI compensator.

$$G_{i,ol}(s) = \left(K_{pi} + \frac{K_{ii}}{s}\right)\frac{1}{L_f s + R_f}\frac{1}{T_{\mathrm{PWM}}s + 1}$$

where TPWM is time delay of switching frequency of the modified PWM; Kpi and Kpi are the PI compensator's parameters for the inner current loop; Lf and Rf are the inductance and resistance filter components of the converter, respectively. Tuning current compensator is achieved by using modulus optimum technique [26]. The concept of modulus optimum is defined as shifting the dominated poles that cause slow dynamic response and achieving unity gain for the closed-loop system. The PI controller's zero will cancel the pole dominated by the RL circuit dynamics. The open-loop transfer function becomes

$$G_{iol}(s) = \frac{1}{sT_{\mathrm{PWM}}(T_{\mathrm{PWM}}s + 1)}$$

by choosing the following parameters: Kpi = Lf TPWM , Kii = Rf TPWM . One of the advantage of the proposed HBC-based PV station is to generate a supported reactive power to the main grid. The controlling design of the reactive power loop is explained in details. The delivered reactive power of the HBC at PCC is calculated as:

$$Q_{pcc} = -\frac{3}{2}V_{sd}i_q$$

where Vsd is the projection of the ac voltage component on d axis of the stationary reference frame; iq is the projection of the output current of HBC on q reference frame. The open loop transfer function of the reactive power controller is given as follow:

$$G_{ol}(s) = G_Q(s)G_{pi}(s)G_{sw}(s)G_i(s)$$
$$= \left(\frac{3}{2}V_{sd}\right)\left(\frac{k_{pQ}s + k_{iQ}}{s}\right)\left(\frac{1}{T_{\mathrm{PWM}}s + 1}\right)\left(\frac{1}{L_f s + R_f}\right)$$

where τQ is the time constant of the resultant closed-loop system. A general form of the second order system. The frequency of natural oscillation is to be equal

$$\omega_n = \sqrt{\frac{1}{T_{\mathrm{PWM}}\tau_Q}}$$
$$\zeta = \sqrt{\frac{\tau_Q}{4T_{\mathrm{PWM}}}}.$$

Assuming there is no switching power loss, the steady-state operation of power balance relationship of the three-phase HBC is given as:

$$P_{\mathrm{pv}} = P_{\mathrm{cap}} + P_{\mathrm{dc}} + P_{\mathrm{ac}}$$
$$P_{\mathrm{ac}} = \frac{3}{2}V_{sd}i_d$$

where id and Vsd are the projections of the ac current and grid voltage space vectors on the d-axis. The power relationship is further expressed as follows.

$$P_{\mathrm{cap}} = CV_{\mathrm{dc}}\frac{dV_{\mathrm{dc}}}{dt} = P_{\mathrm{pv}} - P_{\mathrm{ac}} - P_{\mathrm{dc}}$$
$$= V_{\mathrm{dc}}I_{\mathrm{pv}} - \frac{3}{2}V_{sd}i_d - V_{\mathrm{dc}}I_{\mathrm{dc}}$$

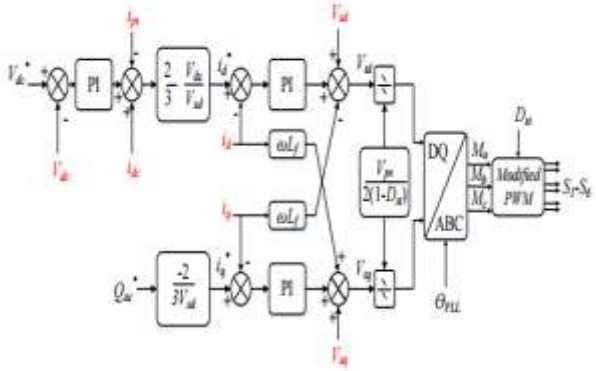

Fig.6. Vector control scheme of the three-phase HBC.

Therefore, the dynamics of the capacitor voltage can be expressed as follows.

$$C\frac{dV_{\mathrm{dc}}}{dt} = \underbrace{I_{\mathrm{pv}} - \frac{3}{2}\frac{V_{sd}}{V_{\mathrm{dc}}}i_d - I_{\mathrm{dc}}}_{u_d}$$

A negative feedback controller will be designed to take in the dc voltage error V ∗ dc−Vdc and amplified by a PI controller. The output of the PI controller is ud. From this signal, the reference signal i ∗ d will be generated as:

$$i_d^* = \frac{2}{3}\frac{V_{\mathrm{dc}}}{V_{sd}}(u_d - I_{\mathrm{pv}} + I_{\mathrm{dc}}).$$

The open-loop transfer function of outer voltage is given as:

$$G_{v,ol}(s) = \left(K_{pv} + \frac{K_{iv}}{s}\right)\frac{1}{\tau_i s + 1}\frac{1}{Cs}$$

where τi is the time constant for the inner current closed loop. The open-loop transfer function for voltage controller includes two poles at origin. Symmetrical optimum is a technique to deal with an open loop system with double integrators [26]. The concept of symmetrical optimum is to operate the system at a low frequency to slow down the dynamic response which leads to an increased phase margin. The compensator parameters are given based on the symmetrical optimum method as follows. where τi is the time constant for the inner current closed loop. The open-loop transfer function for voltage controller includes two poles at origin. Symmetrical optimum is a technique to deal with an open loop system with double integrators [26]. The

concept of symmetrical optimum is to operate the system at a low frequency to slow down the dynamic response which leads to an increased phase margin. The compensator parameters are given based on the symmetrical optimum method as follows.

$$T_{iv} = a^2\tau_i, \quad K_{pv} = \frac{C}{K\sqrt{T_{iv}\tau_i}}, \quad K_{iv} = \frac{K_{pv}}{T_{iv}}$$

where K equals 3Vsd 2Vdc and a is the symmetrical frequency range between peak phase margin and low frequency operation area. It is important to select a high value of the symmetrical gain a to achieve high phase margin. The value of a falls between 2 and 4 [27].

4.SIMULATION STUDIES AND . EXPERIMENTAL RESULTS

Case studies for a PV charging station using a three phase HBC with the proposed control are conducted in MATLAB/Sim Power Systems environment. The data for the PV model are based on PV array type Sun power SPR-E20-327. The V-I and P-V curves for different irradiance values are shown in Fig. 5. The battery parameters of Chevrolet Volt and Nissan Leaf are used to represent the batteries of PHEVs [6], [35], [36].

Case 1: Performance of the Modified Incremental Conductance-PI MPPT

The goal of this case study is to validate the performance of the modified MPPT using incremental conductance-PI algorithm. According to Fig. 5, the maximum PV power is 100 kW when the PV array generates 273.5 V at 1 kW/m2 solar irradiance. Fig. 7shows the performance of MPPT when the system is subject to solar irradiance variation.

The dc voltage Vdc and the PV voltage Vpv are related based on the duty cycle ratio Dst that is generated from MPPT. The role of vector controller is to keep the dc voltage Vdc at its reference value 350V and supply reactive power Q∗ ac to the ac grid. The role of MPPT algorithm is to adjust the duty cycle ratio Dst and in turn adjust the PV output voltage Vpv so that the PVs are operating at the maximum power extracting point.

Fig. 7 provides the performance of MPPT based on four different intervals. From 0−0.5 seconds, the sun irradiance is 0.9 kW/m2 and the MPPT control is not activated. The output PV power supplies approximately 70 kW. At t = 0.5 seconds, MPPT is activated, the duty cycle ratio is decreased and the PV voltage is improved. This in turn improves the PV power output to be 90 kW. Note that whether the MPPT is on or off, Vdc is kept at 350 V.

At t = 1 second and t = 1.5 seconds, the sun irradiance increases and decreases. Due to the MPPT control, the optimal PV output voltage is kept at the optimal level. Further, the PV output power tracks the maximum point at each irradiance level.

Fig. 7 validates the good tracking performance of MPPT when different solar irradiations are applied to the PV. The simulation results also show that the vector controller can regulate the dc voltage at 350 V and reject disturbances.

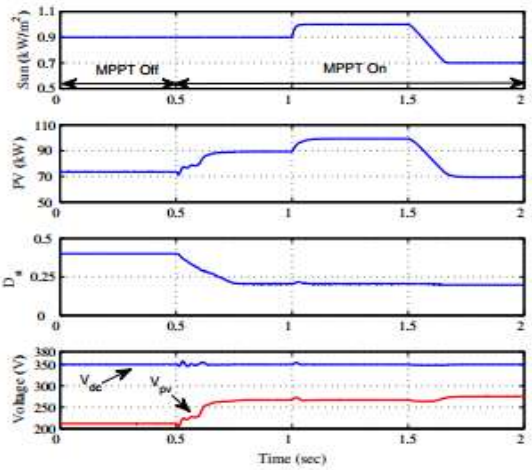

Fig.7. Performance of a modified IC-PI MPPT algorithm when solar irradiance variation is applied.

Case 2: Performance of reactive power control

Another advantage of the three-phase HBC control is that it can support the ac grid by supplying or absorbing reactive power. The vector controller of PV charging station using three-phase HBC is well designed in previous sections to achieve decouple controlling for real and reactive power. This feature is applied in this case study to investigate the ability of the vector controller to quickly track the reactive power reference as well as maintain a constant dc voltage.

The system is first in steady-state and the vector controller regulates the dc voltage and supply ac power at unity power factor as shown in Fig.8. At t = 0.5 seconds the reference reactive power absorbs 10 kVAr while at t = 1 seconds it is changed to supply 20 kVAr to the main ac grid. The controller shows a good performance to track the reactive power reference as well as regulate the dc voltage at 350 V. Fig.8 illustrates that the vector controller's Md and Mq respond to the reactive power variation as well as main a constant dc voltage. It also shows that the dc voltage and reactive power can be controlled independently.

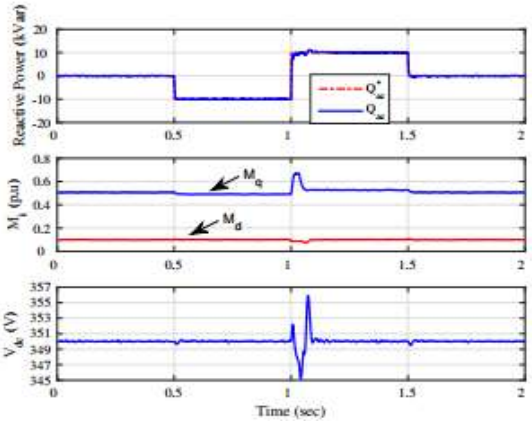

Fig.8. Performance of a proposed vector control to supply or absorb reactive power independently.

Case 3: Partial grid failure

The controller design of the three-phase HBC based PV charging station can take care of the partial grid failure. The controller is designed to provide a stable dc voltage even when grid fault is occurred. Generally, when the main grid voltage sages below 80% of the nominal voltage, the power quality standards recommend to disconnect the charged PHEV to protect the battery's life cycle [37]. The goal of designing the PV charging station's controller is to achieve constant charging procedure when a fault is occurring at the main grid. The method of is to provide sufficient power to charge the PHEV's batteries as well as to maintain a constant dc-link voltage. As a result, it is unnecessary to disconnect the PHEVs during grid fault. The capability of partial grid failure tolerance is demonstrated in the following case study.

The PV charging station is first connected to the main grid where the PHEV's batteries are charged during the steady-state period. MPPT is enabled at t = 0.5 seconds. A symmetrical 70% voltage sag is occurred at t = 1.0 seconds. Normally, it is recommended to disconnect the ac load as well as the PHEV's batteries for protection and safety. However, the proposed controller can mitigate this issue by stabilizing the dc-link voltage at its rated value as well as generating the required power to the local ac load. As can be seen in Fig. 20, the controller of the PV charging station can stabilize the dc bus voltage at its rated value. As shown in Fig. 20, the generated real power from the PV station (Ppv) is kept the same (100 kW) due to MPPT control. The PHEV load (60 kW) is kept the same since the dc-bus voltage is kept the same. In turn, the power right after the HBC PHBC to the ac side is kept the same (40 kW). The 70% reduction in the ac voltage reduces the load power consumption from 20 kW to decreased to 10 kW. In turn, the power to the grid Pac is increased to 30 kW. At t = 1.5 seconds, the voltage recovers to 1 pu and the powers return to the values before 1 seconds.

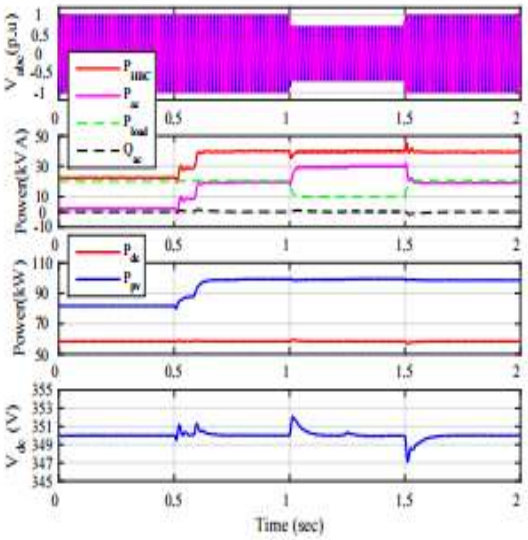

Fig.9. System performance under 70% grid's voltage drop.

The behavior of the proposed PHEV charging station has been validated using a laboratory prototype. National Instruments (NI) Single-Board RIO-9606 and a NI General Purpose Inverter Controller (GPIC) are used to validate the topology of the HBC-based PV charging station. The Lab View field programmable gate array (FPGA) performs signal processing, data analysis, and system controlling using a host computer. The system's controller is implemented using Lab View-FPGA to drive the switches of the HBC as well as monitor the charging procedure of the battery. It also provides a system's protection by monitoring the thermal behavior of the HBC as well as disconnecting the battery when a fault occurs. NI-GPIC board measures the real-time data of the power inverter and executes the controlling signals. The exchanged information between the host application on Lab View-FPGA and the NIGPIC is realized by Ethernet network.

A laboratory PHEV charger is constructed to validate the topology and operation of the system in this paper. For safety reasons, the power rating is downscaled due to the limitation of the actual battery and the NI-GPIC. Fig. 10shows the laboratory setup of the PHEV charging station. The layout of the experimental testing is categorized into five main parts, including NI Single-Board GPIC RIO-9606, NIGPIC back-back inverters, a host Lab View-FPGA computer, dc power supply, and dc and ac loads. The NI-GPIC back-back inverters contain two inverters which are used for the HBC topology and off-board dc/dc converter. The configuration of the HBC requires adjusting the topology of the NI-GPIC back inverters since the research board contains only three phase IGBT-based inverters. The detailed configurations of the HBC and off-board converters are given in Fig.11. The dc load contains Lithium-ion battery which mimics the PHEV's battery. Sinopoly SP-LFP40AHA Lithium-ion battery is used for the experimental testing which is connected to the off board

dc/dc converter for performing a charging procedure. The programmable dc source is used for replacing the PV power source. The ac output filter contains LC components to filter out the high-frequency components of the output signals. The ac side is connected to a resistive load RL

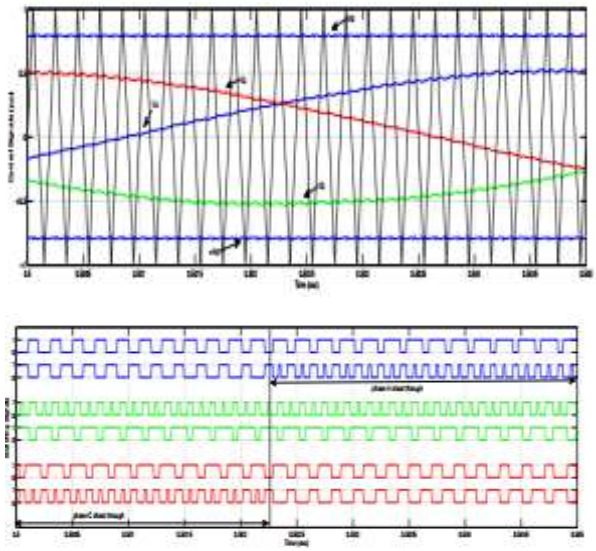

Fig. 10. The modified PWM signals and the switching sequences.

5 . CONCLUSION

Control of three-phase HBC in a PV charging station is proposed in this paper. The three-phase HBC can save switching loss by integration a dc/dc booster and a dc/ac converter into a single converter structure. A new control for the three-phase HBC is designed to achieve MPPT, dc voltage regulation and reactive power tracking. The MPPT control utilizes modified incremental conductance-PI based MPPT method. The dc voltage regulation and reactive power tracking are realized using vector control. Five case studies are conducted in computer simulation to demonstrate the performance of MPPT, dc voltage regulator, reactive power tracking and overall power management of the PV charging station. Experimental results verify the operation of the PHEV charging station using HBC topology. The simulation and experimental results demonstrate the effectiveness and robustness of the proposed control for PV charging station to maintain continuous dc power supply using both PV power and ac grid power.

REFERENCES

[1] M. Ehsani, Y. Gao, and A. Emadi, Modern electric, hybrid electric, and fuel cell vehicles: fundamentals, theory, and design. CRC press, 2009.

[2] K. Sikes, T. Gross, Z. Lin, J. Sullivan, T. Cleary, and J. Ward, "Plugin hybrid electric vehicle market introduction study: final report," Oak Ridge National Laboratory (ORNL), Tech. Rep., 2010.

[3] A. Khaligh and S. Dusmez, "Comprehensive topological analysis of conductive and inductive charging solutions for plug-in electric vehicles," IEEE Transactions on Vehicular Technology, vol. 61, no. 8, pp. 3475– 3489, 2012.

[4] T. Anegawa, "Development of quick charging system for electric vehicle," Tokyo Electric Power Company, 2010.

[5] F. Musavi, M. Edington, W. Eberle, and W. G. Dunford, "Evaluation and efficiency comparison of front end ac-dc plug-in hybrid charger topologies," IEEE Transactions on Smart grid, vol. 3, no. 1, pp. 413– 421, 2012.

[6] F. Musavi, W. Eberle, and W. G. Dunford, "A high-performance single phase bridgeless interleaved PFC converter for plug-in hybrid electric vehicle battery chargers," *IEEE Trans. Ind. Electron.*, vol. 47, no. 4, pp. 1833–1843, Aug. 2011.

[7] F. Musavi, W. Eberle, and W. G. Dunford, "A phase shifted semi bridge less boost power factor corrected converter for plug-in hybrid electric vehicle battery chargers," in *Proc. IEEE Appl.* Power *Electron. Conf. Expo.*, Fort Worth, TX, Mar. 2011, pp. 821–828.

[8] B. Singh, B. N. Singh, A. Chandra, K. Al-Haddad, A. Pandey, and D. P. Kothari, "A review of single phase improved power quality AC–DC converters," *IEEE Trans. Power Del.*, vol. 50, no. 5, pp. 962–981, Oct. 2003.

[9] D. C. Erb, O. C. Onar, and A. Khaligh, "Bi-directional charging topologies for plug-in hybrid electric vehicles," in *Proc. IEEE Appl. Power Electron.Conf. Expo.*, Feb. 21-25, 2010, pp. 2066–2072.

AUTHOR'S PROFILE:

[1]. CH.SURESH KUMAR Pursuing his Masters Degree in Department of EEE from Kakinada Institute Of Technological Sciences (Kits), Ramachandrapuram.

[2]. N.S.KALYAN CHAKRAVARTHI received his Bachelors of Engineering from Andhra University, Vishakhapatnam and Masters Degree from JNTU Kakinada. Presently He is working as Head of the Department & Associate Professor, Department of EEE, in Kakinada Institute of Technological Sciences, Ramachandrapuram (Affiliated to JNTU Kakinada), Andhrapradesh, India. He has 4 International Journal Publications and 21 national publications. His research interest include power quality , power system dynamics and stability and fact devices.